Available online at www.sciencedirect.com
ScienceDirect
Ceramics International 33 (2007) 1563–1567
CERAMICS INTERNATIONAL
www.elsevier.com/locate/ceramint

Sintering of MgO-based refractories with added WO_3

Bingqiang Han [a,*], Yousheng Li [a], Chengcheng Guo [a], Nan Li [a], Fangyu Chen [b]

[a] *The Hubei Province Key Laboratory of Refractory and Ceramics, Wuhan University of Science and Technology, Wuhan Hubei 430081, PR China*

[b] *Wuhan Iron and Steel Company, Wuhan Hubei 430081, PR China*

Received 11 October 2005; received in revised form 25 May 2006; accepted 2 July 2006
Available online 24 October 2006

Abstract

The effects of WO_3 on properties of MgO-based refractories were studied and microstructures analyzed using scanning electron microscopy (SEM) and EDS. WO_3 can improve the sintering of MgO-based refractories. <2 wt% WO_3 is favorable to improve the cold modulus of rupture of MgO-based refractories, but high levels of WO_3 have a negative effect on cold MOR and thermal shock. The low melting phases $MgWO_4$ and $CaWO_4$ formed in MgO boundaries result in increased liquid volume. The formation of $CaWO_4$ leads to C/S ratio change and decreased levels of C_3S and C_2S, and the low melting phase CMS forms. Thus, the densification is improved by phase liquid sintering. SEM observation confirms the existence of $CaWO_4$ and $MgWO_4$ grain boundary phases.

Keywords: D. MgO; Liquid sintering; Microstructure

1. Introduction

With high melting point, chemical stability in a basic environment, magnesia-based refractories, are widely used in cement rotary kilns, and steel ladle, and converters. However, they do have shortcomings, such as high thermal conductivity and poor infiltration resistance. Chemical corrosion, and infiltration loosen the magnesia aggregates and lead to spalling [1]. Much research has aimed to improve corrosion, especially infiltration, and resistance. The trends to more severe environment for high-quality products mean that magnesia-based refractories potentially have wider application, if their shortcomings can be overcome. Flake graphite was introduced because of its low wettability to melting slag [2]. Microsilica (SiO_2), microalumina (Al_2O_3), zirconia (ZrO_2), Cr_2O_3, and other oxides have also been introduced to improve infiltration resistance [3–11]. Furthermore, the introduction of Si^{4+}, Ti^{4+}, Zr^{4+}, and Cr^{3+} ions is thought to enhance the sintering of magnesia and densification.

Sintering of high purity magnesia is related to its impurity content, the ratio of CaO/SiO_2 and the distribution of silicate phases. Generally, liquid phases formed at grain boundaries are the main cause of sintering. Minor cation additions, such as Al^{3+}, Ti^{4+}, Fe^{3+}, Cr^{3+}, and Mn^{2+} are effective in reducing the sintering temperature believed due to nonstoichiometry of periclase caused by crystal lattice defects [4–9]. Second phase formed at grain boundaries also facilitates sintering. For example, the enhancement of densification of MgO by TiO_2 can be rationalized on the basis of cation vacancy formation as follows [5,8]:

$$TiO_2 \xrightarrow{MgO} Ti_{Mg}^{\cdot} + V_{Mg}^{''} + 2O_o$$

When excess TiO_2 exceeds the solid solubility limit, it reacts with magnesia to form intergranular and intragranular magnesium titanate (Mg_2TiO_4), which promotes magnesia grain growth [5,8]. The sintering mechanisms in magnesia are a result of several factors. WO_3 is widely used in electronics, cemented carbide and catalyst as an important raw material. Generally, tungsten has series sub-oxides, which are categorized into WO_{3-x} [12,13]. The MgO–WO_3 and CaO–WO_3 binary diagrams show formation of $MgWO_4$ and $CaWO_4$, both of which are low melting phases [14]. No similar work has been reported on the sintering and microstructure development of magnesia with added WO_3. This paper describes the effect of addition of WO_3 on the sintering behavior of MgO-based refractories.

* Corresponding author. Fax.: +86 027 6886 2121.
E-mail address: hbqyang@yahoo.com.cn (B. Han).

0272-8842/$32.00
doi:10.1016/j.ceramint.2006.07.014

2. Experimental procedures

Industrial fused magnesia (MgO:97.02; SiO_2:0.46; Al_2O_3:0.21; Fe_2O_3:0.63; CaO:0.78; ignition loss:0.40) and yellow tungsten oxide (purity: $WO_3 > 99.65\%$) were used as the main raw materials. Magnesia with various particles and WO_3 fine powder (d50 = 16 μm) with 0, 2, 4, and 6 wt% were mixed together for 1 h. Mixed materials were then pressed into 25 mm width, 25 mm tall, and 125 mm long in briquettes at a pressure of 100 MPa. All the pressed samples were dried at 110 °C for 24 h and sintered at 1100, 1300, 1400, 1500, and 1600 °C at a heating rate of 5 °C/min and a soaking period of 3 h at the designed temperature. Phase composition was analyzed by X-ray diffraction using Cu Kα radiation (model Philips X'pert pro). Densification was studied by measuring bulk density and linear shrinkage. Three briquettes (25 mm × 25 mm × 125 mm) were used to evaluate modulus of rupture (MOR) at both ambient and elevated temperature, respectively. Retention of cold MOR after thermal shock was measured to appraise the thermal shock resistance (four cycles of 30 min heating at 1100 °C and 10 min of subsequent water quenching). Microstructure of the composite was observed by scanning electron microscopy (SEM) (model Philips XL30 TMP) with attached energy dispersive analysis (EDAX Phoenix) for semi quantitative elemental analysis.

3. Results and discussion

3.1. Bulk density and apparent porosity

Fig. 1(a and b) gives the relationship of apparent porosity and bulk density with WO_3 addition and firing temperature. At 1100 °C, with increased WO_3, the bulk density of the batches increases gradually but the bulk density has a minimum value of 2.57 g/cm^3. It is shown that addition of WO_3 has no obvious effect on the apparent porosity of the batch sintered at 1100 °C, but has great effect on those sintered at 1400, 1500, and 1600 °C, which reach a minimum with 2 wt % WO_3 at 1600 °C. The apparent porosity decreases from 21.2% on addition of 0 wt% WO_3 to 18.2% on addition of 2 wt% WO_3, which is associated with higher extent of sintering and higher sintering temperatures, no significant variation in bulk density is observed. WO_3 has a beneficial effect on the sintering of the MgO, especially for the 1600 °C sintered samples.

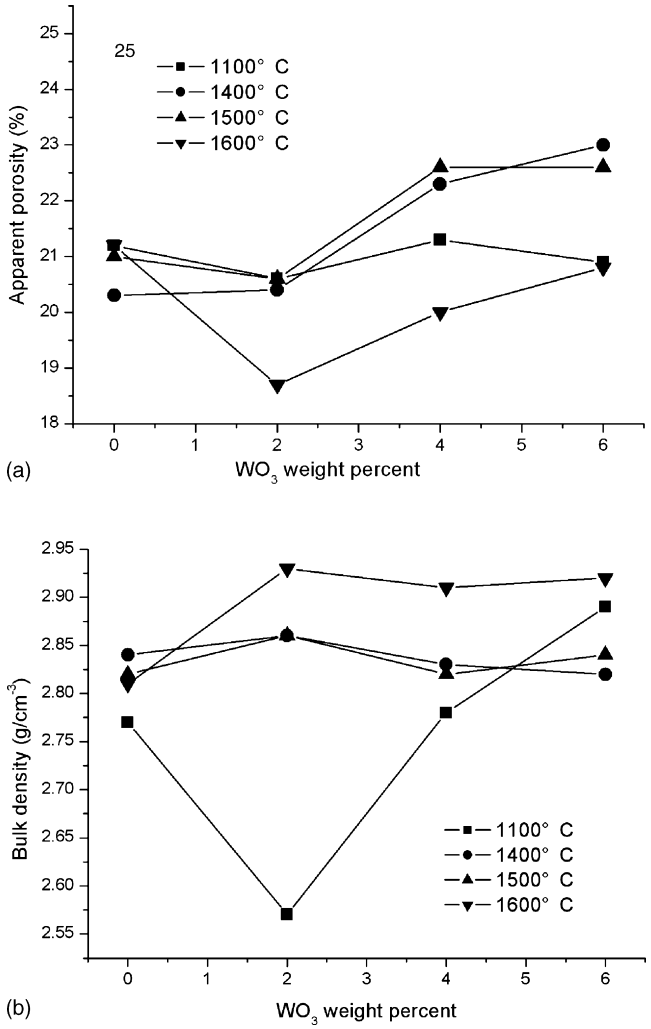

Fig. 1. Variation of (a) apparent porosity and (b) bulk density with WO_3 addition and firing temperature.

3.2. Linear shrinkage

Fig. 2 gives linear shrinkage at various temperatures indicating the extent of sintering. For the samples soaked at 1100 °C, linear shrinkage varies a little with the addition of WO_3. However, with increased WO_3 content, linear shrinkage decreases and expansion is observed for samples with more than 2 wt% WO_3 soaked at 1400 and 1500 °C. The expansion offsets the shrinkage and inhibits densification. For samples soaked at 1600 °C, while linear shrinkage also decreases with increased addition of WO_3, it is always above 0.3%. Pore coalescence at higher temperature may be responsible for this phenomenon. From above mentioned, it can be concluded that 2 wt% WO_3 is an effective sintering aid at 1600 °C.

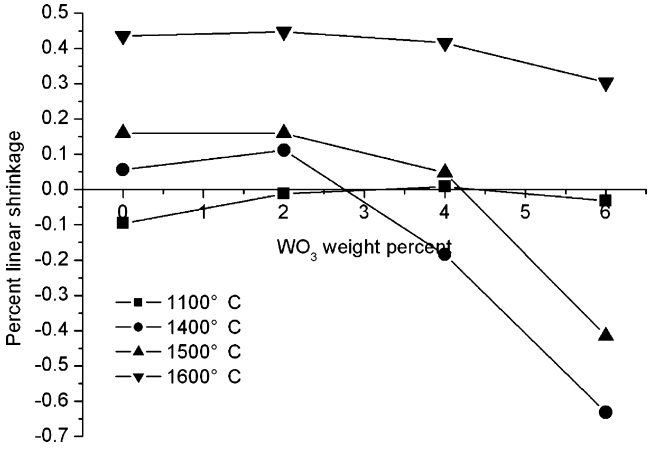

Fig. 2. Variation of permanent linear change with WO_3 addition.

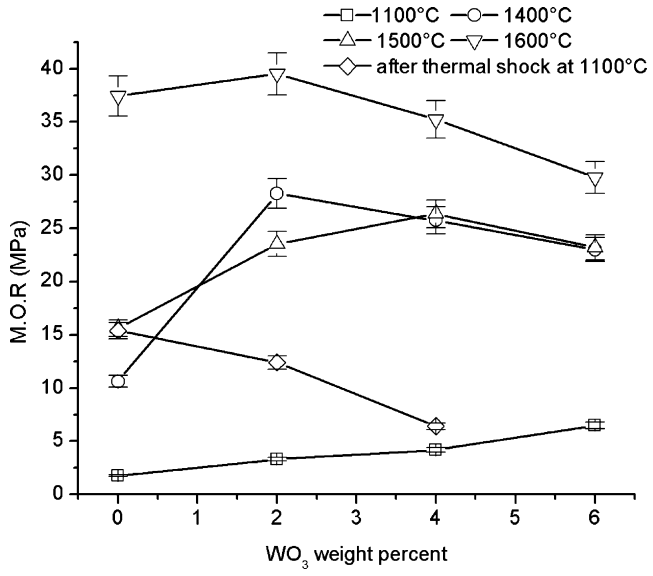

Fig. 3. Variation of cold modulus of rupture with WO_3 addition.

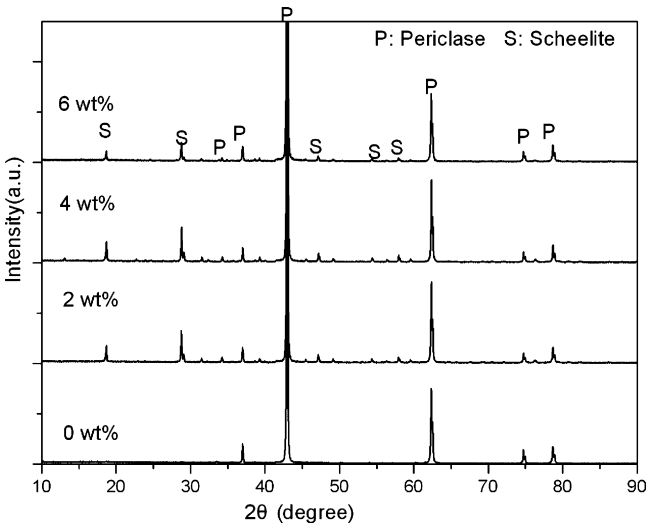

Fig. 4. XRD of the samples containing different level of WO_3 after soaking at 1600 °C.

3.3. MOR and thermal shock

Fig. 3 gives the cold modulus of rupture (MOR) after soaking at various temperatures with different levels of WO_3 addition. For comparison, the residual MORs of the samples after four thermal cycles at 1100 °C are also plotted. Fig. 3 reveals that cold MORs at 1100 °C remains nearly unchanged with increasing WO_3 content. However, after soaking at 1400, 1500, and 1600 °C, cold MOR reaches a maximum with 2 wt% WO_3 and there is a fall when the WO_3 content is above 2 wt%. More WO_3 confers no improvement on MOR. From the dependence of cold MOR on WO_3 content and firing temperature, cold MOR increases with increased firing temperature. The extent of thermal shock damage is determined by retention of cold MOR after different numbers of thermal cycles. A gradual degradation of strength with increasing numbers and WO_3 content is observed. All samples are broken after four thermal cycles. WO_3 has a detrimental effect on strength retention.

3.4. Formation of new phases

Fig. 4 shows XRD with various amounts of WO_3 after soaking at 1600 °C for 3 h. For comparison, the pure magnesia material without WO_3 is also plotted. With no WO_3, only periclase is detected and $3CaO{\cdot}SiO_2$ (C_3S) or $2CaO{\cdot}SiO_2$ (C_2S) do not occur, which are usually the main bond phases. However, when the amount of WO_3 rises from 0 to 6 wt%, $CaWO_4$ (scheelite) appears, its level increasing with WO_3 content. Note that at 6 wt% WO_3 $CaWO_4$ content reduces.

3.5. Microstructure

Generally, the microstructure of fused magnesia varies with purity. Continuous or isolated silicate phases are found at magnesia grain boundaries, which have important effects on magnesia-based refractory products [15]. The phase composition of the silicate, $3CaO{\cdot}SiO_2$, $2CaO{\cdot}SiO_2$, or $CaO{\cdot}MgO{\cdot}SiO_2$(CMS), are determined by the ratio of CaO/SiO_2. Fig. 5 shows the microstructure of 2 wt% WO_3 sample heated at 1600 °C. Table 1 shows the EDS from the points in Fig. 5. Element W is not found in the MgO particles but found at boundaries of the MgO particles. The existence of W can be judged by high contrast of the micrographs in back-scattered electron image mode. There are two possible existing forms. $CaWO_4$ is formed by WO_3 reacting with CaO (points 1–3), which has a continuous structure with thickness of about 2–3 μm. The other phase is $MgWO_4$ formed by WO_3 reacting with MgO. The possible phases in points 4 and 5 are $CaWO_4$, C_3S, and CMS. The main elements at

Table 1
EDS of points in Fig. 5

	O_K (wt%)	Mg_K (wt%)	Si_K (wt%)	Ca_K (wt%)	W_L (wt%)	Possible phases
1	10.22			13.9	75.88	$CaWO_4$
2	10.5			15.00	74.24	$CaWO_4$
3	13.22			16.02	70.75	$CaWO_4$
4[a]	24.78	4.87	1.86	22.4	46.1	$CaWO_4$ + $MgWO_4$ + C_3S(m) + CMS(m)
5	15.07	1.93	8.26	42.74	32.00	$CaWO_4$ + $MgWO_4$ + C_3S(m) + CMS(m)
6	30.24	1.65	16.47	51.64		C_2S

Error range for EDS data is about 5%.
[a] $CaWO_4$ is major phase; $MgWO_4$, C_3S and CMS are minor phases.

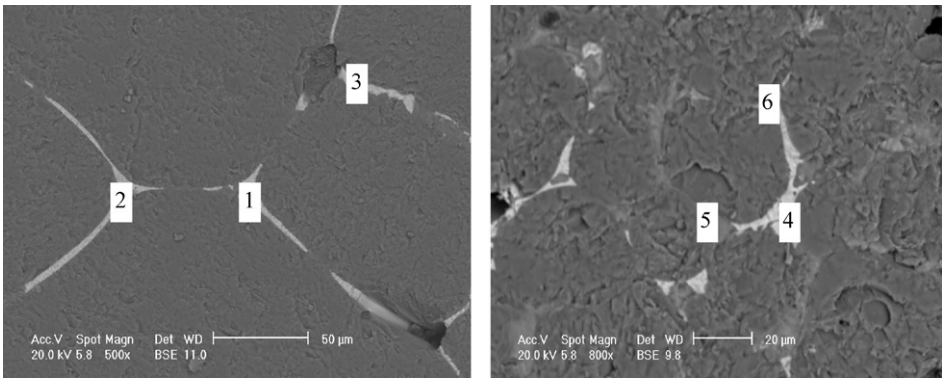

Fig. 5. SEM photographs in back-scattered electron image mode of containing 2 wt% WO_3 sample fired at 1600 °C for 3 h, showing the distribution of secondary phases in triple junctions and the isolated pockets of bright liquid confirming the presence of $CaWO_4$.

point 6 are Ca, Si, and O of approximately to the composition of C_2S. From the above analysis, it can be concluded that $MgWO_4$ and $CaWO_4$ formed at the boundaries of the MgO particles when WO_3 was added into MgO based refractories as additives.

3.6. Discussion

The densification of MgO by TiO_2 is believed due to the lattice defect and formation of Mg_2TiO_4, which prompts grain growth of MgO [5,8].

The densification of MgO refractories with added WO_3 may be due to liquid phases, lattice defects and formation of $CaWO_4$ and $MgWO_4$.

No literatures have discussed the defect of MgO doped by WO_3. Since no W is found in the MgO particles by EDS, so the densification caused by defect is not being confirmed. Thus, the densification is mainly caused by liquid phases. WO_3 will react with MgO and CaO at grain boundaries and the possible reactions take place as follows:

$$WO_3 + MgO = MgWO_4$$

$$WO_3 + CaO = CaWO_4$$

According to the thermochemical data, the standard Gibbs free energy of the first reaction at 25 °C is −71.27 kJ/mol and the second is −149.01 kJ/mol [16,17]. In other words, these reactions can take place but the second is more likely and stable than the first. So $CaWO_4$ forms firstly. If there is WO_3 left, $MgWO_4$ will form. The melting point of the former phase is 1380 °C and the latter is 1580 °C. Although the existence of $MgWO_4$ in these samples was not detected by XRD, however, the synthesis of $MgWO_4$ by solid-state reaction of MgO and WO_3 at about 1100–1200 °C has been reported [14,18,19]. $MgWO_4$ has two distinct polymorphs as α-$MgWO_4$ and β-$MgWO_4$. α-$MgWO_4$ with a triclinic structure is a high temperature phase existing only at 1250 °C, while β-$MgWO_4$ with a monoclinic structure is stable at low temperature [14,18,19]. α-$MgWO_4$ decomposes to MgO and liquid at about 1380 °C.

The formation of $CaWO_4$ leads to C/S ratio change and decreased levels of high melting C_3S and C_2S phases but the low melting phase CMS forms. $CaWO_4$, $MgWO_4$ and CMS are not high melting phases and coexist in the form of continuous liquid at 1600 °C. The liquid phase penetrates MgO grain boundaries. Therefore, more pores in the MgO refractories may become filled with liquid, MgO particles will rearrange. The liquid sintering is enhanced and promotes the densification of magnesia. Therefore, the WO_3 was advantageous to the sintering of the magnesia.

4. Conclusions

WO_3 is found to improve the sintering of MgO-based refractories especially at 1600 °C. The low melting phases $MgWO_4$, $CaWO_4$, and CMS formed in MgO boundaries resulting in increased liquid volume and improved densification. <2 wt% WO_3 is favorable to improving the cold modulus of rupture of MgO-based refractories, but higher levels of WO_3 have a negative effect on cold MOR and thermal shock.

Acknowledgements

This work is supported by the funds of ''The Hubei Province Key Laboratory of Refractory and Ceramics, Wuhan University of Science and Technology'', ''Hubei Province Education Branch'' and ''Wuhan Chenguang Plan''.

References

[1] T. Matsui, K. Hiragushi, T. Ikemoto, K. Sawano, A consideration on corrosion of magnesia refractory brick by silicate slag, Taikabutsu 54 (2) (2002) 67–71.
[2] W.E. Lee, S. Zhang, Melt corrosion of oxide and oxide-C refractories, Int. Mater. Rev. 44 (1999) 77–104.
[3] S. Zhang, N.J. Marriott, W.E. Lee, Thermochemistry and microstructures of MgO–C refractories containing various antioxidants, J. Eur. Ceram. Soc. 21 (2001) 1037–1047.
[4] V. Martinac, M. Labor, N. Petric, Effect of TiO_2, SiO_2 and Al_2O_3 on properties of sintered magnesium oxide from seawater, Mater. Chem. Phys. 46 (1996) 23–30.
[5] M. Chaudhuri, G. Banerjee, A. Kumar, S.L. Sarkar, Secondary phases in natural magnesite sintered with addition of titania, ilmenite and zirconia, J. Mater. Sci. 34 (1999) 5821–5825.
[6] T.C. Yuan, G.V. Srinivasan, J.F. Jue, A.V. Virkar, Dual-phase magnesia–zirconia ceramics with strength retention at elevated temperatures, J. Mater. Sci. 24 (11) (1989) 3855–3864.

[7] A. Nishida, S. Fukuda, Y. Kohtoku, K. Terai, Grain size effect on mechanical strength of MgO–ZrO_2 composite ceramics, J. Ceram. Soc. Jpn. 100 (2) (1992) 191–195.
[8] Y.B. Lee, H.C. Park, K.D. Oh, et al., Sintering and microstructure development in the system MgO–TiO_2, J. Mater. Sci. 33 (1998) 4321–4325.
[9] Zh. Chen, Effect of Cr_2O_3 on properties of refractories, Refractories 25 (6) (1991) 352–358 (in Chinese).
[10] O. Masakazu, Y. Syouk, et al., Characteristics of MgO–ZrO_2 raw materials, Taikabutsu 44 (7) (1992) 427.
[11] Y. Hideo, N. Hitoshi, et al., Development of magnesia–zircon castable for steel ladle slag line, Taikabutsu 45 (8) (1993) 491–492.
[12] Y. Wang, Zh. Chen, Y. Li, et al., Electrical and gas-sensing properties of WO_3 semiconductor material, Solid-State Electron. 45 (2001) 639–644.
[13] G. Centi, Other catalytic properties, Catal. Today 56 (2000) 443–453.
[14] J.R. Günter, M. Amberg, "High-temperature" magnesium tungstate, $MgWO_4$, prepared at moderate temperature, Solid State Ionics 32–33 (Part 1) (1989) 141–146.
[15] Zh. Gao, Z. Ping, Zh. Zhang, Microstructure of Refractories, Metallurgy Industry Press, Beijing, 2002, p. 6 (in Chinese).
[16] Y. Liang, Practical Inorganic Thermodynamics Manual Data, Northwest University Press, Shenyang, PRC, 1993, p. 8 (in Chinese).
[17] Q. Guo, O.J. Kleppa, Enthalpies of formation from the component oxides of $MgWO_4$, $CaWO_4$ (scheelite), $SrWO_4$, and $BaWO_4$, determined by high-temperature direct synthesis calorimetry., Thermochim. Acta 288 (1–2) (1996) 53–61.
[18] G. Blassea, G.J. Dirksena, M. Hazenkampa, J.R. Günter, The luminescence of magnesium tungstate dihydrate, $MgWO_4{\cdot}2H_2O$, Mater. Res. Bull. 22 (6) (1987) 813–817.
[19] J.P. Chu, I.J. Hsieh, J.T. Chen, M.S. Feng, Growth of $MgWO_4$ phosphor by RF magnetron sputtering, Mater. Chem. Phys. 53 (1998) 172–178.